PREPARATION OF BIODEGRADABLE CARBOXYMETHYL CELLULOSE-BASED HYDROGELS AND THEIR DUAL APPLICATION IN FERTILIZER CONTROLLED RELEASE AND CATIONIC DYE REMOVAL

LOUBNA DAOUD and SADJIA BENNOUR

Laboratory of Polymer Materials, Faculty of Chemistry, University of Sciences and Technology, Houari Boumediene, BP 32, El Alia, Algiers, 16111, Algeria
✉ *Corresponding author: S. Bennour, sadjiabennour@yahoo.fr*

Contamination of the environment by agrochemicals and organic dyes has become a serious issue. In the current study, bioadsorbents based on carboxymethyl cellulose have been synthesized by performing graft copolymerization of crosslinked poly(acrylamide-co-maleic acid) chains onto carboxymethyl cellulose. The synthesized hydrogels were characterized by FTIR, XRD, SEM and TGA. The swelling properties showed that the hydrogels exhibited thermo- and pH-responsive behavior. The incorporation of fertilizer (ammonium nitrate) into the hydrogel at the time of synthesis was carried out. The fertilizer release mechanism followed the Fickian transport model. The toxic cationic dye (methylene blue) removal study was carried out in dye contaminated aqueous solution at neutral pH. The adsorption kinetics fitted well with the pseudo-second order model. The mechanism of the adsorption process was determined from the intra-particle diffusion model. The aim of this work has been to predict the possibility of using the prepared hydrogels in agriculture and wastewater treatment.

Keywords: carboxymethyl cellulose, hydrogel, swelling, fertilizer release, cationic dye adsorption

INTRODUCTION

Hydrogels may be conveniently defined as chemically or physically crosslinked natural or synthetic polymers.[1] Under physiological conditions, they have the ability to swell and hold a large amount of liquids. Moreover, they are designed to respond to external stimuli, namely pH, temperature, and ionic strength.[2-4]

Hydrogels have gained an extensive popularity as promising materials, in controlled release systems, due to their great potential of sustainable release of the entrapped molecules.[5]

In the agricultural field, controlled release systems based hydrogels have proved many benefits over the conventional systems for fertilizer release, by reducing the negative impact associated with the overdosing usage of fertilizers and increasing the efficiency and sustainability of nutrients supply, owing to the gradual release of these nutrients.[6,7]

The large utilization of organic dyes in industrial production affects not only water quality, but also the color of wastewater. In order to minimize environmental pollution, cross-linked hydrogels with functional groups, such as amine, hydroxyl and carboxyl, are widely employed as adsorbents for the treatment of dye-containing wastewaters.[8,9] Also, they could make a great contribution to saving aquatic life since most dyes are hardly biodegradable.[10]

Due to their important biocompatibility, non-toxicity and excellent hydrophilicity, natural polymers, such as cellulose, starch and chitosan, have attracted great attention in the elaboration of biopolymer based hydrogels.[11-13] Carboxymethyl cellulose (CMC) is a cellulosic derivative that shows good chemical reactivity and higher adsorption capacities due to the presence of hydrophilic groups in its anionic linear polymer chain. It is an important industrial biopolymer that is used in many fields – medicine, food, cosmetics and textiles – as an emulsion stabilizer, viscosity modifier, or water binder agent.[14]

CMC based hydrogels have attracted growing research interest, and their application in the agricultural field and the treatment of dye-containing wastewater from the textile industry has become very promising.[15,16] Hydrophilic monomers are usually utilized to modify CMC through graft copolymerization, in order to improve the polyelectrolyte character of the obtained hydrogels.[17]

The aim of this work has been to prepare a series of biodegradable thermo- and pH-sensitive grafted hydrogels based on acrylamide (AAm) and maleic acid (MA), and to evaluate their potential in the controlled release of fertilizers and the removal of cationic dye. The effects of pH and temperature on the swelling properties of the hydrogels were studied. The model fertilizer, ammonium nitrate, was loaded into the grafted hydrogels by free radical polymerization, and the fertilizer release from the loaded hydrogels was investigated as a function of MA and CMC concentrations. In addition, the kinetics of the removal of methylene blue dye from aqueous solution by the grafted hydrogels was also studied.

EXPERIMENTAL
Materials
The sodium salt of carboxymethyl cellulose (CMC) was purchased from Fluka (Germany), with an average molecular weight of 250000 and degree of carboxyl substitution (DS) of 0.9. Acrylamide (AAm) and maleic acid (MA) were purchased from Fluka (Germany) and employed as monomers. N,N'-methylenebisacrylamide (MBAA; Fluka, Germany), as a cross-linking agent, potassium persulfate (KPS; Merck, Germany), as an initiator, ammonium nitrate (NH_4NO_3; Merck, Germany), as a fertilizer, and methylene blue (MB; Sigma-Aldrich, Germany), as a cationic dye, were used as received.

The pH-buffered solutions were prepared as follows:[18] pH = 2, HCl/KCl, I = 0.06 M ; pH = 4, citric acid/phosphate, I = 0.23 M; pH = 6, citric acid/phosphate, I = 0.38 M; pH = 7, citric acid/phosphate, I = 0.49 M; pH = 9, boric acid/NaOH, I = 0.03 M; pH = 10, boric acid/NaOH, I = 0.15 M.
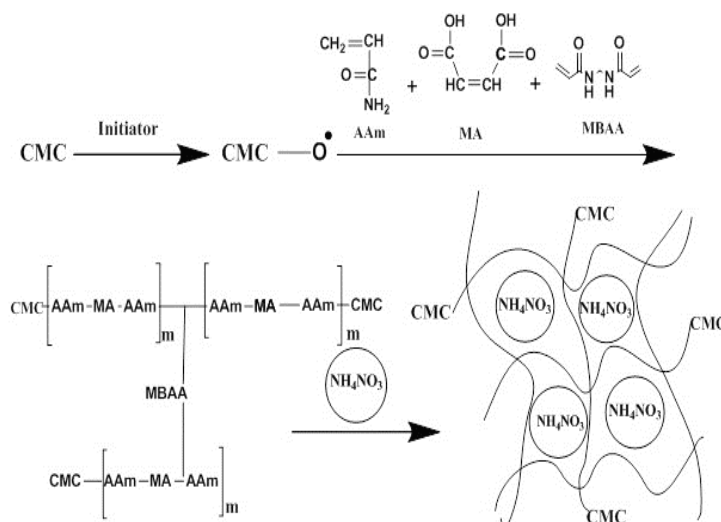
Synthesis of CMC-P(AAm-MA) hydrogels
A determined amount of CMC powder (0.2-0.5 g) was dissolved in 30 mL of distilled water in a 50 mL three-necked flask, equipped with a magnetic stirrer, a reflux condenser and a nitrogen line to obtain a sticky transparent solution. After being purged with nitrogen for 30 min to remove the oxygen dissolved in the solution, the solution was heated to 60 °C and, then, 5 mL of aqueous solution with initiator KPS (0.004 g) was added under continuous stirring for 10 min to generate radicals. Different amounts of AAm and MA monomers and 0.02 g of MBAA were added to the mixture, and the reaction was maintained at 60 °C for 3 h to complete the polymerization process. The nitrogen atmosphere was maintained throughout the reaction period. The resulting gels were cut into small cylinders, washed several times with distilled water, dried at room temperature for several days and, then, in a vacuum oven at 60 °C until constant weight. The details for different hydrogel formulations are given in Table 1.

Table 1
Composition of unloaded CMC-P (AAm-MA) and loaded CMC-P (AAm-MA)/F

Hydrogels	AAm (mmol)	MA (mmol)	CMC[a] (wt%)	NH_4NO_3[a] (wt%)	KPS[b] (mol%)	MBAA[b] (mol%)
CMC-PAAm	41.0	0.0	7	-	0.036	0.32
CMC-P(AAm-MA)-1	36.9	4.1	7	-	0.036	0.32
CMC-P(AAm-MA)-2	32.8	8.2	7	-	0.036	0.32
CMC-P(AAm-MA)-3	28.7	12.3	7	-	0.036	0.32
CMC-P(AAm-MA)-4	32.8	8.2	10	-	0.036	0.32
CMC-P(AAm-MA)-5	32.8	8.2	14	-	0.036	0.32
CMC-P(AAm-MA)-6	32.8	8.2	17	-	0.036	0.32
CMC-P(AAm)/F	41.0	0.0	7	14	0.036	0.32
CMC-P(AAm-MA)/F1	36.9	4.1	7	14	0.036	0.32
CMC-P(AAm-MA)/F2	32.8	8.2	7	14	0.036	0.32
CMC-P(AAm-MA)/F3	28.7	12.3	7	14	0.036	0.32
CMC-P(AAm-MA)/F4	32.8	8.2	10	14	0.036	0.32
CMC-P(AAm-MA)/F5	32.8	8.2	14	14	0.036	0.32
CMC-P(AAm-MA)/F6	32.8	8.2	17	14	0.036	0.32

[a] wt% of the total weight of monomers, [b] mol % of the total mole number of monomers

Scheme 1: Synthesis of fertilizer loaded hydrogel CMC-P(AAm-MA)/F

The grafting reaction can be explained as follows: in the first step, the initiator is decomposed under heating to generate sulfate anion-radicals. The radicals extract hydrogen from the hydroxyl groups in the CMC to form alkoxy radicals on the substrate. Then, the monomer molecules, close to those reaction sites, become acceptors of CMC radicals resulting in chain initiation and, thereafter, they themselves become free radical donors to neighboring molecules. In this way, the grafted chain grows. During the chain propagation, the polymeric chains may react synchronously with the end vinyl groups of MBAA, and finally a cross-linked structure is formed.[19]

Synthesis of fertilizer loaded CMC-P(AAm-MA)/F hydrogels

Details of the synthesis of loaded CMC-P(AAm-MA)/F hydrogels are presented in Table 1. Seven formulations were synthesized by incorporating 0.4 g of ammonium nitrate in each, following the same process for the synthesis of hydrogels as in the absence of fertilizer. After complete mixing of the CMC and monomer solution, an amount of NH_4NO_3 (0.4 g) was added and the mixing operation was continued for 3 h. The produced samples were sliced into cylinders and dried in a vacuum oven at 60 °C until constant weight without washing them. The synthesis route of the fertilizer loaded hydrogel is shown in Scheme 1.

Characterization
Fourier transform infrared spectroscopy (FTIR) measurements

FTIR spectra were recorded on a Perkin Elmer spectrophotometer, at room temperature with a resolution of 2 cm^{-1}, with an average of 60 scans. Spectra were collected in the infrared region of 4000-400 cm^{-1}. Hydrogel samples were ground to a powder, mixed with potassium bromide and pressed into a disk.

Scanning electron microscopy (SEM)

The surface morphology of the dried hydrogels was observed on a JOEL JSM 6360-LV scanning electron microscope instrument after gold coating, operating at the accelerating voltage of 10 kV.

X-ray diffraction (XRD)

X-ray diffraction measurement of the prepared samples was performed on a D8 Advance diffractometer (Bruker) using Cu Kα radiation (λ = 1.54 Å). The X-ray data were recorded in the range from 10° to 60° (2θ).

Thermogravimetric analysis

Thermogravimetric analysis of the CMC-P(AAm-MA) hydrogels was carried out on a TA instrument Q500 under nitrogen atmosphere from 25 °C to 580 °C at a heating rate of 10 °C/min.

Swelling measurements

The gravimetric procedure was utilized for studying the swelling kinetics. Briefly, the dried hydrogel samples of known weights were immersed in buffer solutions at various pH values, ranging from 2 to 10 at 25 °C, and at various temperatures in the range of 25-70 °C at pH = 7. Then, the samples were taken out at desired time intervals, put on filter paper to remove excessive water, and weighed.

The swelling ratio (SR) was calculated from the following equation:

$$SR\ (\%) = [(m_t - m_0)/\ m_0] \times 100 \qquad\qquad (1)$$

where m_0 is the mass of the dry gel and m_t is the mass of the swollen gel at time t. Swelling measurements were done two or three times, and the average values have been reported in the data.

Release of ammonium nitrate

The loaded gels (2-3 mm length) of known weight (0.1 g) were placed in 100 mL of double-distilled water under stirring. The conductivity of the release medium, determined at desired time intervals by using a conductivity meter (INOLAB COND 730), is related to the amount of NH_4NO_3 using a calibration plot. Release measurements were done two or three times and the average values have been reported in the data.

Dye removal experiments

The adsorption behavior of methylene blue onto CMC-P(AAm-MA) hydrogels was investigated by batch adsorption experiments. 50 mg of dried hydrogels, at different ratios of CMC and MA, were placed in 100 mL of 0.1 g/L methylene blue solution and magnetically agitated at moderate speed at 25 °C. A small quantity of dye solution was withdrawn at fixed periods of time. Measurements of MB concentration were performed using a UV-VIS spectrophotometer (UV-3100PC-VWR) at 664 nm. The procedure was carried out in triplicate and the average was taken.

The adsorption capacity q_t (mg/g) was calculated according to the following equation:

$$q_t = [(C_0 - C_t) / m] \times V \qquad (2)$$

where C_0 and C_t (mg. L^{-1}) are dye concentrations at initial time and at time t, respectively; m is the weight of adsorbent (g) and V is the volume of dye solution (L).

RESULTS AND DISCUSSION
FTIR spectral analysis

Figure 1a shows the infrared spectra of CMC, CMC-PAAm and CMC-P (AAm-MA) in the 3900-2200 cm^{-1} region. In the FTIR spectrum of CMC, a broad band centred at 3480 cm^{-1} is due to the stretching frequency of the OH groups. The shoulder at 3250 cm^{-1} is related to the intra-chain hydrogen bonds.[20] The FTIR spectrum of CMC-PAAm reveals a broad absorption band at 3490 cm^{-1}, corresponding to the overlap of N-H stretching of the AAm unit and O-H stretching band of the CMC portion of the homopolymer. A shoulder at 3184 cm^{-1} is attributed to asymmetrical N-H stretching. Introducing MA units into the CMC-PAAm backbone is accompanied with the gradual shift of the band at 3490 cm^{-1} to lower wavenumbers of 3480 cm^{-1}, indicating the formation of hydrogen bonding interactions between the carbonyl groups of AAm and the hydroxyl groups of MA. Also, the shoulder at 3184 cm^{-1} shifts to 3191 cm^{-1}.

The infrared spectra of CMC, CMC-PAAm and CMC-P (AAm-MA), in the carbonyl region, are depicted in Figure 1b. The FTIR spectrum of CMC shows the bands at 1614 cm^{-1} and 1425 cm^{-1}, associated with the carboxylate anion, and the peak at 1072 cm^{-1}, assigned to the -C-O-C- ether ring. Additionally, a small peak observed around 1727 cm^{-1} is related to the carboxylic groups.[21] The spectrum of CMC-PAAm marks the presence of a band at 1660 cm^{-1} and a peak at 1400 cm^{-1}, related to the amide group and the carboxylate anion, respectively. The shoulder at 1752 cm^{-1} is due to the carboxylic groups of CMC. On the other hand, we notice a shift of the band at 1668 cm^{-1}, ascribed to hydrogen bonding between carboxyl and amide groups, to lower wavenumbers of 1663 cm^{-1} with the increase in the MA amount within the CMC-P(AAm-MA) copolymer.

In the hydroxyl stretching region, the infrared spectra of CMC-P(AAm-MA) with different CMC compositions are illustrated in Figure 1c. With increasing the CMC content in the copolymer, the band at 3486 cm^{-1}, characteristic of the carboxyl-carbonyl amide interactions, shifts to 3484 cm^{-1}. The shift of the band at 2520 cm^{-1}, assigned to dimeric acid, to lower wavenumbers – 2467 cm^{-1} – is also observed.

The infrared spectra of unloaded CMC-P(AAm-MA)-2 and loaded CMC-P(AAm-MA)/F2, in the 2000-900 cm^{-1} region, are given in Figure 1d. With the incorporation of NH_4NO_3 into the hydrogel matrix, the band related to carboxyl-carbonyl amide interactions shifts from 1667 cm^{-1} to 1657 cm^{-1}. In addition, the shoulder and the band at 1607 cm^{-1} and 1457 cm^{-1} shift to lower wavenumbers – 1602 cm^{-1} and 1421 cm^{-1}, respectively. Also, the shift of the peak at 1740 cm^{-1}, corresponding to the free carboxyl groups, to 1716 cm^{-1} is attributed to hydrogen bonding between the hydroxyl group of MA and the unpaired electrons on oxygen atoms of NH_4NO_3.[22] In addition, the peak observed at 1320 cm^{-1} corresponds to the nitrate ion.[23] This indicates the entrapment of NH_4NO_3 in the hydrogel matrix.
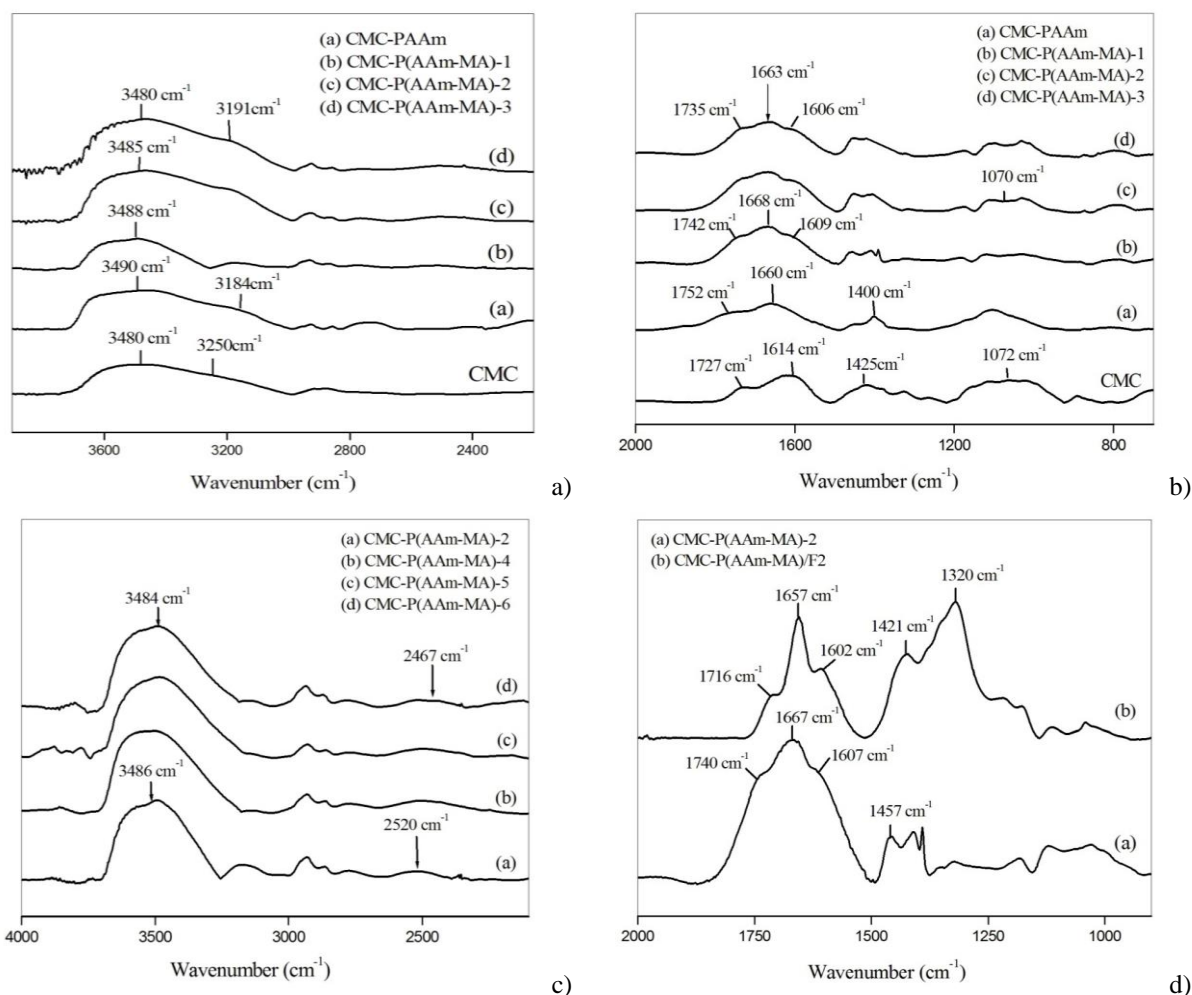
Figure 1: FTIR spectra of CMC-P (AAm-MA) hydrogels (a) in the hydroxyl region, (b) in the carbonyl region, (c) with different compositions of CMC in the hydroxyl region, (d) unloaded CMC-P (AAm-MA)-2 and loaded CMC-P (AAm-MA)/F2 in the carbonyl region

SEM

The surface appearance of CMC and dried hydrogels was observed using the SEM technique and the obtained images are illustrated in Figure 2. For pure CMC, the SEM image shows an irregular and clumped surface morphology (Fig. 2a). The SEM micrograph of the CMC-PAAm homopolymer exhibits an undulant and coarse surface, with some cracks over it (Fig. 2b), while the surface morphology of grafted copolymers appears to be smooth and tight, without any fractures or pores (Fig. 2c and 2d).

XRD

Figure 3a displays the XRD patterns of CMC, CMC-PAAm and CMC-P (AAm-MA) copolymers. The XRD pattern of CMC shows a diffraction peak at $2\theta = 20.8°$, indicating its semi-crystalline nature. The peak of CMC shifted to $2\theta = 23.7°$ in the pattern of the CMC-PAAm homopolymer, suggesting the rupture of hydrogen bonds between the molecular chains of CMC, and thus resulting the loss of crystallinity. Incorporating MA within the CMC-PAAm backbone tends to shift this peak to $2\theta = 22.9°$.

Thermogravimetric analysis

The thermogravimetric (TGA) and derivative thermogravimetric (DTGA) curves of CMC, CMC-PAAm and CMC-P(AAm-MA) with different amounts of MA are represented in Figure 3b. The parameters, such as temperature of maximum degradation (determined considering the derivative curves), percentage of mass loss in each stage of degradation and percentage of solid residue for all studied systems, are gathered in Table 2.

The pure CMC degrades in three main stages. The first stage, located between 50 °C and 220 °C, corresponds to the removal of free water (below 100 °C), absorbed water (below 160 °C) and partial oxidation of OH groups to COOH groups (below 220 °C).[20,24] The breaking of cellulose chains into smaller units occurs in the second stage from 235 °C to 335 °C. The last step is related to dehydration, depolymerization and pyrolytic decomposition.[25] The thermal degradation of CMC-PAAm occurs in three stages. In the initial stage, the weight loss of about 7%, from 162 to 235 °C, is associated with absorbed water. The second stage, from 237 to 300 °C, is due to the loss of ammonia with the formation of imide groups via cyclization.[26] The third stage, at a temperature higher than 301 °C, is attributed to the process accompanying main chain scission.

The CMC-P(AAm-MA)-1 copolymer degrades in three stages. The first step corresponds to desorption of moisture as hydrogen bonded water molecules to the hydrophilic groups. In the second stage, the formation of a ring structure among the imide groups takes place. The main chain scission process occurs in the third stage. For CMC-P(AAm-MA)-2 and CMC-P(AAm-MA)-3, two thermal stages are observed. The percentage of mass loss in the range 15-18%, in stage 1, is apparently associated with absorbed water by the hydrophilic groups and anhydride formation.[27] The second stage corresponds to the effective degradation of the copolymers.

As shown in Table 2, it can be noticed that the temperature of maximum degradation of CMC-P(AAm-MA) decreases with increasing CMC amount, in the second step of degradation. In other words, the thermal stability of CMC-P(AAm-MA)-6 is lower as compared to that of the other copolymers.
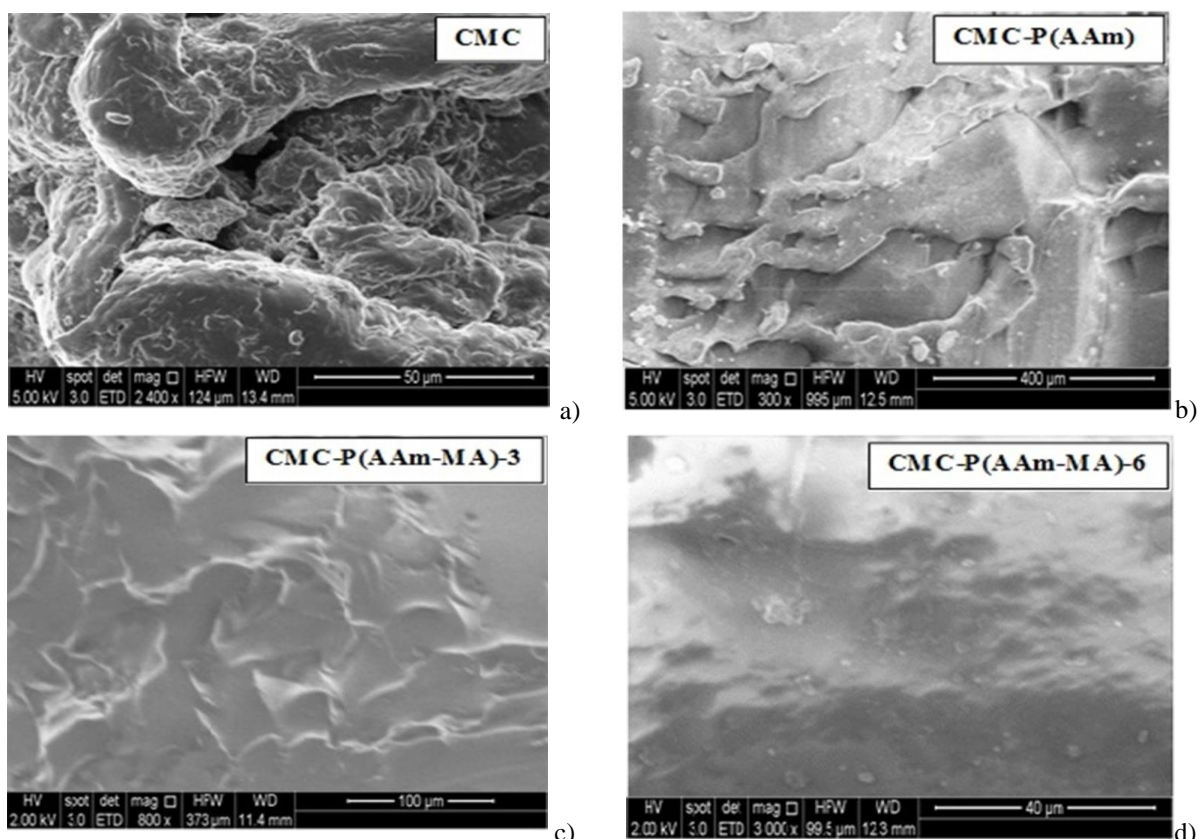

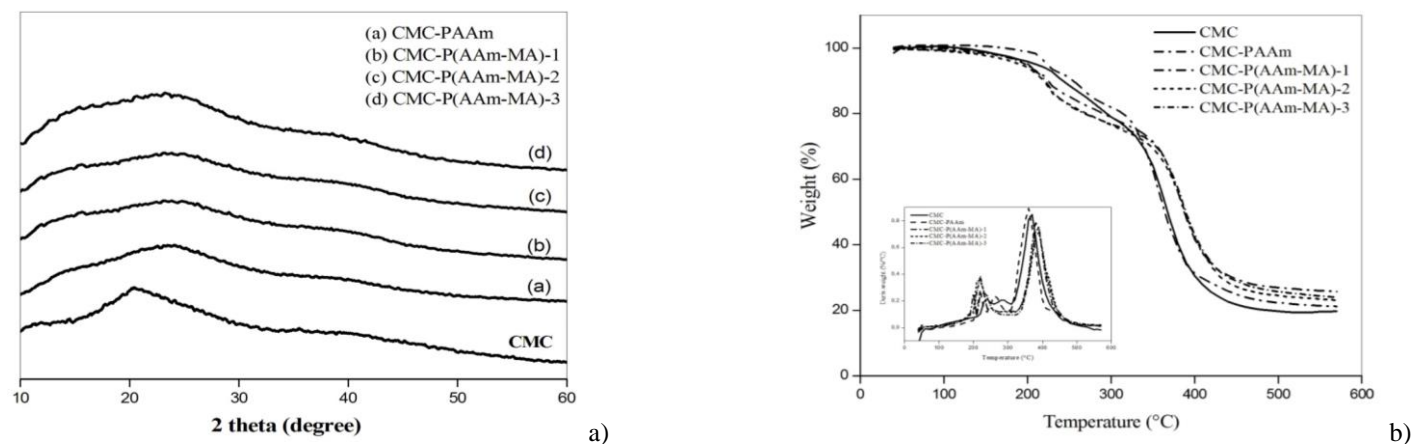Figure 2: SEM images of (a) pure CMC, (b) CMC-PAAm, (c) CMC-P (AAm-MA)-3, (d) CMC-P (AAm-MA)-6

Figure 3: (a) XRD patterns for original CMC and CMC-P (AAm-MA) hydrogels with various amounts of MA; (b) TGA thermograms and DTGA curves of CMC-P (AAm-MA) hydrogels with different amounts of MA

Table 2
Thermogravimetric parameters of CMC-P (AAm-MA) hydrogels

Hydrogels	Stage 1			Stage 2			Stage 3			Residual weight (wt%)
	ΔT^a (^{o}C)	Δm^b (wt%)	T^c_{max} (^{o}C)	ΔT^a (^{o}C)	Δm^b (wt%)	T^c_{max} (^{o}C)	ΔT^a (^{o}C)	Δm^b (wt%)	T^c_{max} (^{o}C)	
CMC	50-220	7	-	235-335	41	290	340-510	11	-	41
CMC-PAAm	162-235	7	220	237-300	12	263	301-483	59	359	22
CMC-P(AAm-MA)-1	141-211	6	203	212-290	13	225	293-495	53	383	26
CMC-P(AAm-MA)-2	157-278	15	233	285-496	59	391	-	-	-	24
CMC-P(AAm-MA)-3	131-281	18	231	285-497	54	387	-	-	-	25
CMC-P(AAm-MA)-4	144-278	19	226	283-495	56	389	-	-	-	23
CMC-P(AAm-MA)-5	140-269	17	221	271-496	56	374	-	-	-	24
CMC-P(AAm-MA)-6	149-272	17	224	277-495	50	371	-	-	-	32

[a] Temperature range; [b] Total weight loss percentage at the end of the step; [c] Temperature maximum values of DTGA curves

Swelling analysis

Effect of maleic acid

Figure 4a displays the swelling ratio of CMC-P (AAm-MA) hydrogels, with different maleic acid contents, at pH 7 and 25 °C. As can be seen, the CMC-P (AAm-MA)-2 gel exhibits a higher swelling ratio. Raising the MA content from 4.1 to 8.2 mmol in the hydrogel results in an enhanced swelling capacity. When the MA content is further increased, the hydrogen bonding density of the network becomes so high that the diffusion of water molecules into the polymeric matrix is restrained, thus implying a lower swelling ratio.

Effect of CMC content

The effect of CMC concentration on the swelling of CMC-P(AAm-MA) copolymers at pH 7 and at 25 °C was investigated by varying the CMC amount in the range of 7-17 wt% in the gel. As seen from Figure 4b, when the concentration of CMC is increased in the hydrogel, the swelling ratio is found to decrease. Increasing the CMC content enhances the crosslinking with the polymer matrix, thus restricting the relaxation of the polymer matrix and the diffusion of water.
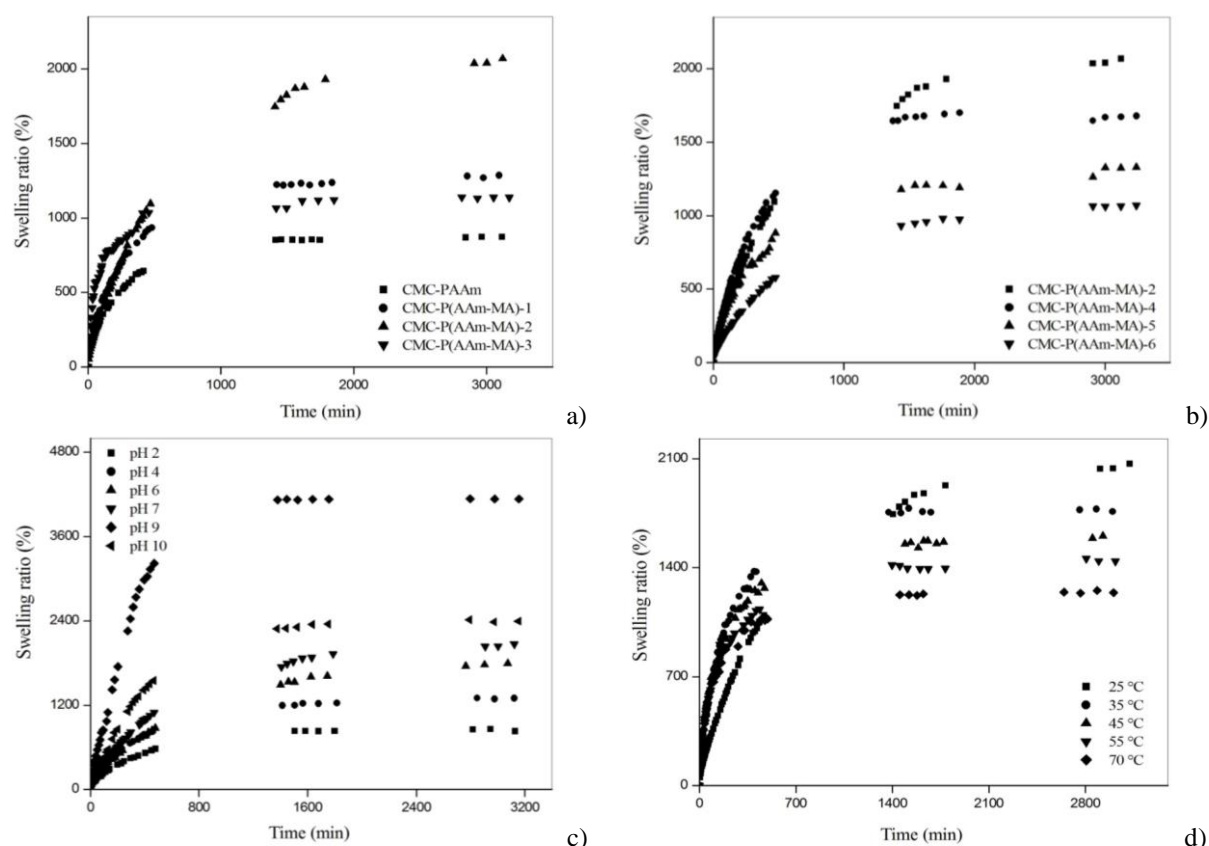

Figure 4: (a) Effect of MA content on the swelling behavior of CMC-P (AAm-MA) hydrogel in the medium of pH 7 at 25 °C; (b) Effect of CMC content on the swelling behavior of CMC-P (AAm-MA) hydrogel in the medium of pH 7 at 25 °C; (C) Effect of pH on the swelling ratio of CMC-P (AAm-MA)-2 hydrogel at 25 °C; (d) Effect of temperature on the swelling ratio of CMC-P (AAm-MA)-2 hydrogel at pH 7

Effect of pH

The influence of pH on the swelling of CMC-P(AAm-MA)-2 copolymer at 25 °C was investigated and the results are shown in Figure 4c. It is clear from the figure that the maximum extent of swelling is reached at pH 9. At pH values lower than the pKa value of maleic acid, the first and second dissociation constants of MA are $pKa_1 = 1.85$ and $pKa_2 = 6.06$, respectively,[28] most of the carboxylate groups are protonated and converted to carboxylic acid groups, leading to a decrease of the swelling ratio. At higher pHs, the carboxylic groups are ionized and, consequently, the electrostatic repulsion between -COO$^-$ groups increased. So, the polymer network tends to swell more. Beyond the pH value

of 9, a drop in the swelling ratio is related to the increase of ionic concentration in the external medium.[29]

Effect of temperature

The effect of temperature on the swelling ratio of CMC-P(AAm-MA)-2 hydrogel is illustrated in Figure 4d. As can be seen, the swelling ratio decreases with the increase in temperature. This suggests that the hydrogen-bonding force between the water and the macromolecular chain is reduced. Then, the bound water becomes non-binding water, free water, which can move rapidly out of the polymeric network, implying shrinkage of the hydrogel. Similar results have also been reported by other researchers.[30]

Ammonium nitrate release

The release of fertilizer from the hydrogel implies the sorption of water into the polymeric matrix and simultaneous release of fertilizer via diffusion. However, the electrostatic repulsion between -COO$^-$ and NO$_3^-$ in the hydrogel and the hydrogen bonds formed between the copolymer chains reduce the migration of fertilizer from the hydrogel. In the following paragraph, the effect of CMC and MA compositions on the release kinetics will be discussed.

In the present study, the concentration of maleic acid has been varied in the loaded copolymer in the range of 4.1-12.3 mmol, and the influence of this variation on the release profiles of NH$_4$NO$_3$ has been evaluated, as depicted in Figure 5a. The results suggest that the released content of NH$_4$NO$_3$ rises with the increase of MA concentration. Increasing the hydrophilic groups in the polymer matrix increases the affinity for water, thus leading to a higher released amount of NH$_4$NO$_3$.

The effect of the CMC content in the loaded CMC-P (AAm-MA)/F hydrogel on its release behavior is shown in Figure 5b, which reveals that the released amount of NH$_4$NO$_3$ increases when the CMC content increases in the feed mixture in the range of 7-14 wt% and, thereafter, decreases. With an increasing amount of CMC, the electrostatic repulsion between -COO$^-$ groups increased, implying the relaxation of the macromolecular chains. This may facilitate the diffusion of water molecules into the polymer matrix, so the released content of NH$_4$NO$_3$ is enhanced. However, beyond 14 wt% of CMC, the electrostatic repulsion between COO$^-$ and NO$_3^-$ increases.[31,32] This obviously results in slow diffusion of water molecules into the hydrogel network and, consequently, the release of NH$_4$NO$_3$ content decreases.

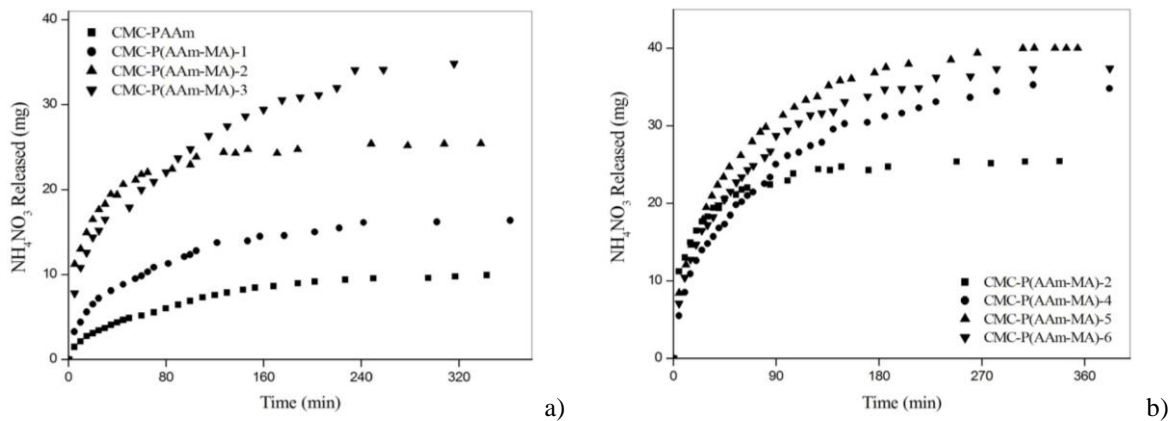Figure 5: (a) Effect of MA content in the loaded hydrogel on the released amount of NH$_4$NO$_3$ at 25 °C; (b) Effect of CMC variation in the loaded hydrogel on the released amount of NH$_4$NO$_3$ at 25 °C

NH$_4$NO$_3$ release dynamics

To determine the nature of NH$_4$NO$_3$ diffusion from the hydrogel, kinetic modelling was conducted based on the Fickian diffusion law for the onset stage of NH$_4$NO$_3$ release.[33,34]

$$\frac{M_t}{M\infty} = kt^n \qquad (3)$$

where M$_t$ and M∞ denote the NH$_4$NO$_3$ content diffused from the hydrogel at time t and equilibrium time, respectively, *k* is a constant related to the structure of the polymer matrix, and the exponent *n* is a

number to determine the type of diffusion. The kinetic parameters n and k would be calculated from the slope and intercept of the plot of ln (Mt/ M∞) vs. ln t.

Normal Fickian diffusion is characterized by n = 0.5, while case II diffusion by n = 1. A value of n between 0.5 and 1 indicates non-Fickian or anomalous diffusion. The corresponding kinetic parameters n and k of CMC-PAAm/F and CMC-P(AAm-MA)/F1 to 6 samples are given in Table 3. The values of diffusional exponent are lesser than 0.5, indicating the release of NH_4NO_3 from the fertilizer loaded hydrogel follows a Fickian diffusion mechanism.

The diffusion coefficient (D) of the fertilizer release from the hydrogels can be calculated from the following equation:[33,34]

$$\frac{Mt}{M\infty} = 4 \left(\frac{Dt}{\pi l^2} \right)^{0.5} \tag{4}$$

where D is the diffusion coefficient and l is the thickness of the sample.

The diffusion coefficient values for ammonium nitrate release from the loaded hydrogels with various CMC and MA contents, evaluated from the slope of the plots of Mt/ M∞ versus $t^{0.5}$, are summarized in Table 3. It is noticed from the table that the diffusion coefficient value increases with the increase in MA content, from 4.1 to 8.2 mmol, in the CMC-P(AAm-MA)/F hydrogel and, thereafter, decreases. On the other hand, when the CMC amount in the loaded copolymer is raised from 7 to 17 wt%, the value of the diffusion coefficient increases up to 10 wt% and, then, decreases. This reflects that the release of NH_4NO_3 from the loaded CMC-P(AAm-MA)/F containing 10 wt% of CMC is faster, as compared to the other gel samples.

Dye adsorption study

In the present work, the influence of maleic acid concentration, carboxymethylcellulose content and contact time on the removal of MB by CMC-P(AAm-MA) was investigated.

Figures 6a and 6b exhibit the adsorption capacities of methylene blue versus contact time at 25 °C. Results show that the dye uptake increases notably in the first 300 min and, then, the adsorption starts to slow down until reaching an equilibrium phase.

Again, the removal of MB dye depends on the MA and CMC concentrations. Indeed, the increase of maleic acid ratio, from 4.1 to 12.3 mmol, in the CMC-P(AAm-MA) copolymer results in an improvement of the adsorption capacity (Fig. 6a). This is mainly attributed to the increase in the number of ionized carboxylic groups, leading to the growth of electrostatic interactions between the cationic groups of the dye and the negative charge of the carboxyl groups in the hydrogel. Once all the active sites are saturated, the adsorption equilibrium is achieved.

Figure 6b demonstrates the adsorption capacity of the CMC-P(AAm-MA) hydrogel versus time for different concentrations of carboxymethylcellulose. As can be seen, the adsorption rises when the amount of CMC increases. According to this result, increasing COO^- groups in the hydrogel provides more adsorption sites for methylene blue molecules, implying an increase in the adsorption capacity of the hydrogels.

Table 3
Release kinetic coefficients of CMC-P (AAm-MA)/F hydrogels

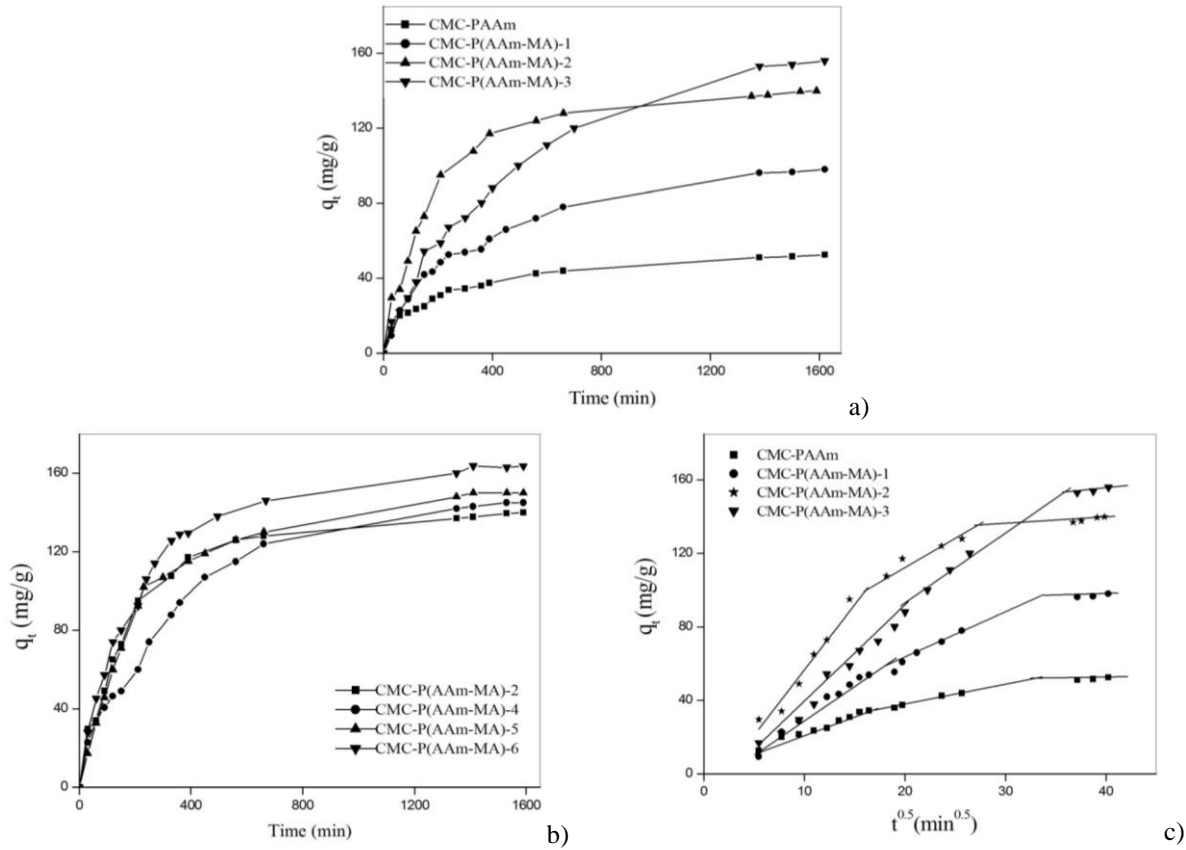| Hydrogels	n	$k \times 10^2$	R^2	$D \times 10^3$ (mm^2/min)	R^2
CMC-PAAm/F	0.50	07.90	0.9993	07.89	0.9993
CMC-(PAAm-MA)/F1	0.44	10.00	0.9944	07.53	0.9960
CMC-(PAAm-MA)/F2	0.45	08.88	0.9969	09.61	0.9962
CMC-(PAAm-MA)/F3	0.37	13.21	0.9989	06.04	0.9952
CMC-(PAAm-MA)/F4	0.48	07.99	0.9919	10.52	0.9954
CMC-(PAAm-MA)/F5	0.42	11.40	0.9916	07.54	0.9904
CMC-(PAAm-MA)/F6	0.45	09.89	0.9955	06.52	0.9946

Figure 6: (a) Effect of MA concentration on adsorption of MB onto CMC-P (AAm-MA) hydrogel at 25 °C; (b) Effect of CMC concentration on adsorption of MB onto CMC-P (AAm-MA) hydrogel at 25 °C; (c) Plots of intra-particle diffusion model for MB adsorption by CMC-P (AAm-MA) hydrogel at different MA compositions

Adsorption kinetic studies

In order to investigate the adsorption process of methylene blue onto CMC-P(AAm-MA) hydrogels, the pseudo-first-order and pseudo-second-order kinetic models were applied to the data obtained from kinetic experiments, and their linear forms are expressed by Equations (5) and (6), respectively:[35,36]

$$\ln(q_e - q_t) = \ln q_{e1} - k_1 t \qquad (5)$$

$$\frac{t}{q_t} = \frac{1}{k_2 q_{e2}^2} + \frac{t}{q_{e2}} \qquad (6)$$

where q_t (mg/g) is the adsorption capacity at any time t (min) and q_e (mg/g) is the adsorption capacity at equilibrium; k_1 (min^{-1}) and k_2 (g/mg min) are the rate constants of the pseudo-first order and pseudo-second order models, respectively.

Kinetic parameters examined in terms of the pseudo-first order and pseudo-second order models were evaluated from the slope and intercept of the linear plots of ln(qe - qt) versus (t) and t/q_t versus (t), respectively. The adsorption kinetic parameters of all the hydrogel samples are listed in Table 4.

It can be ascertained from Table 4 that the calculated correlation coefficient values (R^2) for the pseudo-first order model range between 0.886 and 0.998, suggesting a poor fit of this model to the adsorption data. Also, the calculated q_e values from the pseudo-first order model do not concur with the experimental results. Meanwhile, a straight line with a high correlation coefficient ($R^2 = 0.999$) is obtained in the case of the pseudo-second order model. Again, the equilibrium adsorption capacities (q_{e2}) calculated from the linear plots of pseudo-second order are near to experimental values (q_{exp}). This result implies that the pseudo-second order model could better describe the adsorption process of methylene blue onto CMC-P(AAm-MA) hydrogels.

The pseudo-first order and pseudo-second order kinetic models were not able to explain the diffusion mechanism of the adsorption process. Therefore, the intra-particle diffusion model has been employed to further study the diffusion of MB onto CMC-P (AAm-MA) hydrogels. The linear form of the intra-particle diffusion model can be expressed by the following equation:[37]

$$q_t = k_{id}t^{0.5} + C \qquad\qquad (7)$$

where q_t (mg g^{-1}) is the amount of dye adsorbed at time t, k_{id} is the intra-particle diffusion rate constant (mg/g min$^{0.5}$) and C is related to the boundary layer thickness. The parameters k_{id} and C could be calculated from the slope and intercept of a linear plot of qt versus t$^{0.5}$, respectively. If the intra-particle diffusion is a rate-limiting process, the plot of q_t against t$^{0.5}$ yields a straight line passing through the origin. Otherwise, more steps can influence the adsorption process.

According to Equation (7), the plots of q_t versus t$^{0.5}$ for the adsorption of methylene blue onto CMC-P(AAm-MA) hydrogels with various MA compositions, depicted in Figure 6c, show three linear segments, suggesting that the adsorption of methylene blue occurs in three steps.

A similar three-stage plot has been reported for other dye/adsorbent systems.[38,39] According to the interpretation of this three-stage process, the first stage is assigned to outer diffusion of the dye solution owing to the adsorption sites available on the surface of the hydrogel. The second step can be related to intra-particle diffusion of MB molecules into the interior of the CMC-P(AAm-MA) hydrogels. The third stage is attributed to the equilibrium phase of the adsorption process, reflecting the diminution of dye concentration.[40,41] Moreover, by comparing the intra-particle diffusion rate constants for the hydrogel samples, described in Table 5, we can notice that k_{id} values for the first stage are higher than for the second and third stages. These results can be explained by the availability of a large number of adsorption sites at the initial time, which makes the adsorption rate of methylene blue into CMC-g-P(AAm-MA) hydrogels in this stage faster than in the other stages.

Table 4
Pseudo-first-order and pseudo-second-order rate parameters for MB adsorption
onto CMC-P(AAm-MA) hydrogel

Sample		Pseudo-first order			Pseudo-second order		
	Q_{exp} (mg/g)	Q_{e1} (mg/g)	$k_1 \times 10^3$ (min^{-1})	R^2	Q_{e2} (mg/g)	$k_2 \times 10^5$ (g /mg min)	R^2
CMC-PAAm	52.61	38.41	2.01	0.957	56.49	9.58	0.999
CMC-P(AAm-MA)-1	98.06	78.38	1.90	0.886	114.9	2.64	0.999
CMC-P(AAm-MA)-2	141.7	121.9	3.45	0.994	156.3	2.49	0.999
CMC-P(AAm-MA)-3	156.3	99.42	3.64	0.986	163.9	1.20	0.999
CMC-P(AAm-MA)-4	146.7	136.2	2.49	0.983	175.5	2.21	0.999
CMC-P(AAm-MA)-5	149.8	143.9	4.61	0.996	172.4	2.17	0.999
CMC-P(AAm-MA)-6	163.7	152.8	3.98	0.998	181.8	2.54	0.999

Table 5
k_{id} and correlation coefficient parameters according to intra-particle diffusion model for linear sections

Sample	Intra-particle diffusion model					
	k_{id1} (mg/g min$^{0.5}$)	R^2	k_{id2} (mg/g min$^{0.5}$)	R^2	k_{id3} (mg/g min$^{0.5}$)	R^2
CMC-PAAm	1.85	0.981	1.06	0.991	0.466	0.985
CMC-P(AAm-MA)-1	4.02	0.994	2.52	0.993	0.582	0.929
CMC-P(AAm-MA)-2	4.22	0.994	2.48	0.966	1.010	0.994
CMC-P(AAm-MA)-3	5.13	0.993	3.44	0.995	0.962	0.979
CMC-P(AAm-MA)-4	5.26	0.998	3.78	0.996	0.959	0.996
CMC-P(AAm-MA)-5	8.73	0.996	2.76	0.998	0.641	0.957
CMC-P(AAm-MA)-6	7.70	0.997	2.61	0.994	1.081	0.956

Adsorption mechanism

To determine the nature of interactions between the dye and the CMC-P(AAm-MA) hydrogel, the FTIR spectra of CMC-P(AAm-MA)-3, MB and CMC-P(AAm-MA)-3/MB systems, in the carbonyl region, were investigated and depicted in Figure 7. It can be noticed that the spectra before and after the adsorption of MB greatly changed. The band at 1663 cm^{-1}, corresponding to hydrogen bonding between carboxyl and amide groups, is shifted to 1668 cm^{-1}, after adsorption. A shoulder at 1606 cm^{-1} and a small peak at 1452 cm^{-1}, corresponding to the carboxylate anion, are shifted to 1596 cm^{-1} and 1456 cm^{-1} after adsorption, respectively. A shoulder at 1735 cm^{-1}, assigned to the free carboxyl

groups, disappeared after adsorption. For the loaded CMC-P(AAm-MA)-3/MB, two bands appearing at 1385 cm^{-1} and 859 cm^{-1} are ascribed to bending vibrations of symmetrical –CH3 and out-plane ring (=CH) of MB dye, respectively. The above results indicate that the electrostatic attractions and hydrogen bonding can describe the main adsorption process. Indeed, the available carboxylate groups on the CMC and ionized carboxylic groups of MA developed ionic interactions with the quaternary ammonium groups of MB molecules. Additionally, hydrogen bonding will be expected to occur among nitrogen atoms of amine groups in MB molecules, the hydroxyl groups of CMC and amino groups in PAAm chains.

The mechanism proposed for MB adsorption onto the CMC-P(AAm-MA) hydrogel is illustrated in Scheme 2.
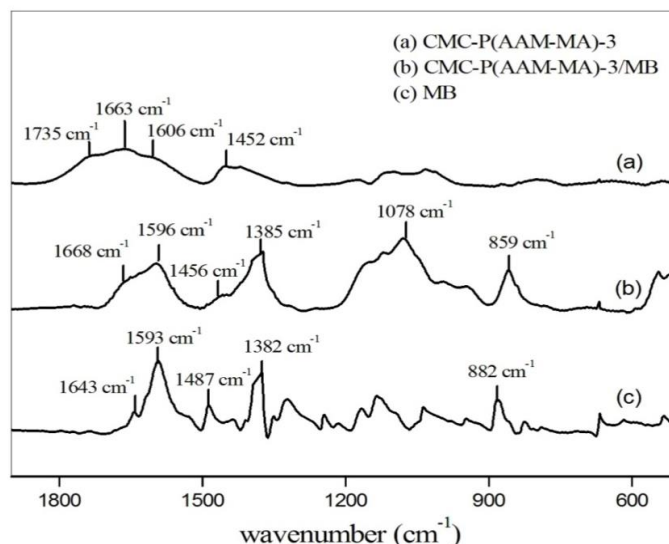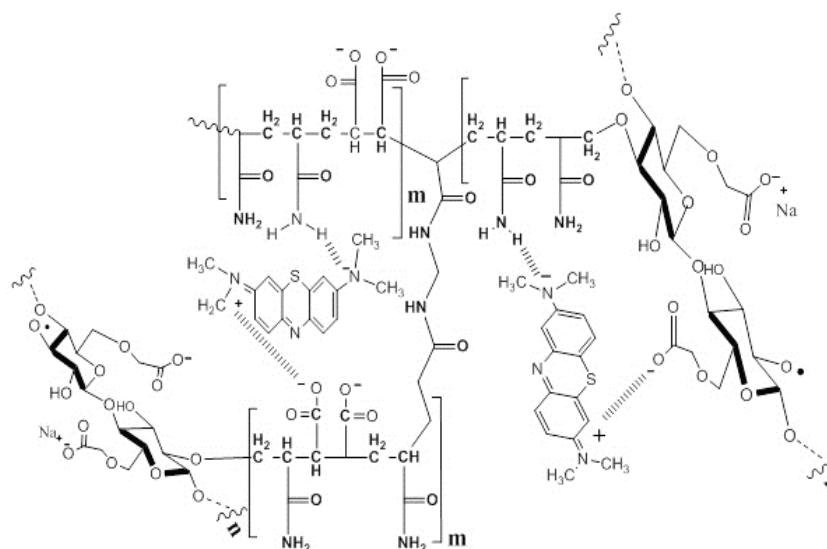

Figure 7: FTIR spectra of MB, CMC-P(AAm-MA)-3 and CMC-P(AAm-MA)-3/MB in the carbonyl region

Scheme 2: Adsorption mechanism of MB onto CMC-P(AAm-MA) hydrogel

CONCLUSION

In this study, CMC-P(AAm-MA) hydrogels were prepared by grafting of AAm and MA on the CMC backbone, using the free radical polymerization technique. FTIR, ATG, XRD and SEM analyses were performed to characterize these gels. Loaded CMC-P(AAm-MA)/F gels were prepared by addition of fertilizer and varying the concentration of MA and CMC. The incorporation of NH_4NO_3 in the hydrogels was confirmed by FTIR. The swelling capacities of the CMC-P(AAm-MA) hydrogels are dependent on pH, temperature and the chemical composition of the gel. The release studies of

NH_4NO_3 show that the release rate is closely related to the concentrations of maleic acid and CMC. The release mechanism follows the Fickian model. The results of the dye adsorption study show that the dye uptake increases with the increase in maleic acid and CMC ratios. The adsorption kinetics is well adjusted by a pseudo-second-order model, and the adsorption mechanism is mainly associated with a three-step intra-particle diffusion process. The prepared hydrogels can be safely used as a fertilizer release agent and as a biosorbent for the removal of dye from wastewater.

REFERENCES

[1] K. Varaprasad, T. Jayaramudu and E. R. Sadiku, *Carbohyd. Polym.*, **164**, 186 (2017), https://doi.org/10.1016/j.carbpol.2017.01.094

[2] F. Andrade, M. M. Roca-Melendres, E. F. Durán-Lara, D. Rafael and S. Schwartz, *Cancers*, **5**, 13 (2021), https://doi.org/10.3390/cancers13051164

[3] H. Zhao and Y. Li, *Colloid Surf. A-Physicochem. Eng. Asp.*, **586**, 124 (2020), https://doi.org/10.1016/j.colsurfa.2019.124270

[4] S. Bennour and F. Louzri, *Adv. Chem.*, **2014**, 1 (2014), https://doi.org/10.1155/2014/147398

[5] X. Lin, Q. Ma, J. Su, C. Wang, R. K. Kankala *et al.*, *Molecules*, **24**, 2089 (2019), https://doi.org/10.3390/molecules24112089

[6] R. Michalik and I. Wandzik, *Polymers*, **12**, 2425 (2020), https://doi.org/10.3390/polym12102425

[7] F. Louzri and S. Bennour, *J. Polym. Mater.*, **37**, 55 (2020), https://doi.org/10.32381/JPM.2020.37.1-2.5

[8] T. T. C. Truong, N. T. T. Vo, K. D. Nguyen and H. M. Bui, *Cellulose Chem. Technol.*, **53**, 573 (2019), https://doi.org/10.35812/CelluloseChemTechnol.2019.53.57

[9] S. Samsami, M. Mohamadi, M. H. Sarrafzadeh, E. R. Rene and M. Firoozbahr, *Process Saf. Environ. Prot.*, **143**, 138 (2020), https://doi.org/10.1016/j.psep.2020.05.034

[10] A. M. Abdel Ghaffar, M. B. El-Arnaouty, A. A. Abdel Baky and S. A. Shama, *Des. Monomer. Polym.*, **19**, 706 (2016), https://doi.org/10.1080/15685551.2016.1209630

[11] M. F. Zaltariov, D. Filip, C. D. Varganici and D. Macocinschi, *Cellulose Chem. Technol.*, **52**, 619 (2018), https://doi.org/10.3390/ijms22052531

[12] Z. Abdollahi, E. N. Zare, F. Salimi, I. Goudarzi, F. R. Tay *et al.*, *Int. J. Mol. Sci.*, **22**, 2531 (2021), https://doi.org/10.3390/ijms22052531

[13] H. Hamedi, S. Moradi, S. M. Hudson and A. E. Tonelli, *Carbohyd. Polym.*, **199**, 445 (2018), https://doi.org/10.1016/j.carbpol.2018.06.114

[14] A. Hebeish, A. Higazy, A. El-Shafei and S. Sharaf, *Carbohyd. Polym.*, **79**, 60 (2010), https://doi.org/10.1016/j.carbpol.2009.07.022

[15] F. Louzri and S. Bennour, *J. Polym. Eng.*, **38**, 437 (2017), https://doi.org/10.1515/polyeng-2017-0074.10.1515/polyeng-2017-0074

[16] N. Pavandi, E. Taghavi and N. Anarjan, *Cellulose Chem. Technol.*, **55**, 375 (2021), https://doi.org/10.35812/CelluloseChemTechnol.2021.55.36

[17] A. V. Sorokin, V. A. Kuznetsov and M. S. Lavlinskaya, *Polym. Bull.*, **78**, 2975 (2021), https://doi.org/10.1007/s00289-020-03250-z

[18] V. Alexeev, "Analyse Qualitative", 4th ed., Mir Publishing House, Moskow, 1980

[19] Y. Bao, J. Ma and N. Li, *Carbohyd. Polym.*, **84**, 76 (2011), https://doi.org/10.1016/j.carbpol.2010.10.061

[20] W. Li, B. Sun and P. Wu, *Carbohyd. Polym.*, **78**, 454 (2009), https://doi.org/10.1016/j.carbpol.2009.05.002

[21] C. Vasile, G. G. Bumbu, R. P. Dumitriu and G. Staikos, *Eur. Polym. J.*, **40**, 1209 (2004), https://doi.org/10.1016/j.eurpolymj.2003.12.023

[22] E. Karadağ, D. Saraydin, Y. Çaldiran and O. Güven, *Polym. Adv. Technol.*, **11**, 59 (2000), https://doi.org/10.1002/(SICI)1099-1581(200002)11:2<59::AID-PAT937>3.0.CO;2-Z

[23] I. Nakagawa and J. L. Walter, *J. Chem. Phys.*, **51**, 1389 (1969), https://doi.org/10.1063/1.1672186

[24] N. S. V. Capanema, A. A. P. Mansur, A. C. de Jesus, S. M. Carvalho, L. C. de Oliveira *et al.*, *Int. J. Biol. Macromol.*, **106**, 1218 (2018), https://doi.org/10.1016/j.ijbiomac.2017.08.124

[25] M. A. Villetti, J. S. Crespo, M. S. Soldi, A. T. N. Pires, R. Borsali *et al.*, *J. Therm. Anal. Calorim.*, **67**, 295 (2002), https://doi.org/10.1023/A:1013902510952

[26] B. R. Nayak and R. P. Singh, *J. Appl. Polym. Sci.*, **81**, 1776 (2001), https://doi.org/10.1002/app.1610

[27] M. Ś. Żeliazkow, *Polym. Degrad. Stab.*, **91**, 1233 (2006), http://dx.doi.org/10.1016/j.polymdegradstab.2005.09.006

[28] R. C. Weast, "Handbook of Chemistry and Physics", The Chemical Rubber Co., Cleveland, Ohio, USA, 53rd ed., 1972, https://doi.org/10.1002/ange.19720840921

[29] C. S. Brazel, and N. A. Peppas, *Macromolecules*, **28**, 8016 (1995), https://doi.org/10.1021/ma00128a007

[30] R. Katiyar, D. S. Bag and I. Nigam, *Adv. Mater. Lett.*, **5**, 214 (2014), http://dx.doi.org/10.5185/amlett.2013.8532

[31] H. Wang, Z. Wang and B. Zhu, *React. Funct. Polym.*, **67**, 225 (2007), https://doi.org/10.1016/j.reactfunctpolym.2006.11.004

[32] L. Daoud and S. Bennour, *Russ. J. Appl. Chem.*, **94**, 1499 (2021), https://doi.org/10.1134/S1070427221110057

[33] P. L. Ritger and N. A. Peppas, *J. Control. Release*, **5**, 23 (1987), http://dx.doi.org/10.1016/0168-3659(87)90034-4

[34] P. L. Ritger and N. A. Peppas, *J. Control. Release*, **5**, 37 (1987), https://doi.org/10.1016/0168-3659(87)90035-6

[35] S. Lagergren, *Kungliga Svenska Vetenskapsakad. Handlingar*, **24**, 1 (1898)

[36] Y. S. Ho and G. McKay, *Chem. Eng. Technol.*, **70**, 115 (1998), https://doi.org/10.1016/S0923-0467(98)00076-1

[37] W. J. Weber and C. J. Morris, in Procs. *1ˢᵗ International Conference on Water Pollution Research*, Oxford, 1962, pp. 231-266

[38] M. Alkan, O. Demirbaş and M. Doğan, *Micropor. Mesopor. Mater.*, **101**, 388 (2007), http://dx.doi.org/10.1016/j.micromeso.2006.12.007

[39] I. A. W. Tan and B. H. Hameed, *J. Appl. Polym. Sci.*, **10**, 2565 (2010), https://dx.doi.org/10.3923/jas.2010.2565.2571

[40] H. Tang, W. Zhou and L. Zhang *J. Hazard. Mater.*, (**209-210**), 218 (2012), https://doi.org/doi:10.1016/j.jhazmat.2012.01.010

[41] S. Rahimi Aqdam, D. E. Otzen, N. M. Mahmoodi and D. Morshedi, *J. Colloid Interface Sci.*, **602**, 490 (2021), http://dx.doi.org/10.1016/j.jcis.2021.05.174